

# Subdwarf B stars from the common envelope ejection channel

H. Xiong<sup>1,2,3</sup> X. Chen<sup>1,2</sup> P. Podsiadlowski<sup>4</sup> and Z. Han<sup>1,2</sup>

<sup>1</sup> Yunnan Observatories, Chinese Academy of Sciences, Kunming 650216, China  
e-mail: cxf@ynao.ac.cn

<sup>2</sup> Key Laboratory for the Structure and Evolution of Celestial Objects, Chinese Academy of Sciences, Kunming 650216, China

<sup>3</sup> University of Chinese Academy of Sciences, Beijing 100049, China

<sup>4</sup> Department of Astrophysics, University of Oxford, Oxford OX1 3RH, UK

Received ...; accepted ...

## ABSTRACT

**Context.** Subdwarf B stars (sdB) are important to stellar evolutionary theory and asteroseismology, and are crucial to our understanding of the structure and evolution of the Galaxy. From the canonical binary scenario, the majority of sdBs are produced from low-mass stars with degenerate cores where helium is ignited in a way of flashes. Due to numerical difficulties, the models of produced sdBs are generally constructed from more massive stars with non-degenerate cores. This leaves several uncertainties on the exact characteristics of sdB stars.

**Aims.** The purpose of this paper is to study the characteristics of sdBs produced from the common envelope (CE) ejection channel.

**Methods.** We use the stellar evolution code *Modules for Experiments in Stellar Astrophysics* (MESA), which can resolve flashes during stellar evolution. To mimic the CE ejection process, we firstly evolve a single star to a position near the tip of red giant branch, then artificially remove its envelope with a very high mass loss rate until the star begins to collapse. Finally, we followed the evolution of the remnant until it becomes a helium or a carbon-oxygen white dwarf.

**Results.** The sdB stars produced from the CE ejection channel appear to form two distinct groups on the effective temperature-gravity diagram. One group, referred as the flash-mixing sdBs, almost has no H-rich envelope and crowns at the hottest temperature end of the extremely horizontal branch (EHB), while the other group, called as the canonical sdBs, has significant H-rich envelope and spreads over the whole canonical EHB region. The key factor for the dichotomy of the sdB properties is the development of convection during the first helium flash, i.e. the convection region penetrates into the H-rich envelope for the flash-mixing sdBs but does not for the canonical sdBs.

**Conclusions.** The dichotomy of the sdB properties from the CE ejection channel is intrinsic and caused by the interior structure of the star after the CE ejection. The modelling of the CE ejection process will change the parameter spaces much for the two typical groups of sdB stars. For a given initial stellar mass and a given core mass at the onset of the CE, if the CE ejection stops early, the star has a relatively massive H-rich envelope, resulting in a canonical sdB generally. The fact of only a few short-orbital-period sdB binaries being in the flash-mixing sdB region and the lack of He-rich sdBs in short-orbital-period binaries indicate that the flash mixing is not very often in the products of the CE ejection. A falling back process after the CE ejection, similar to that happened in nova, is an appropriate way of increasing the envelope mass, then prevents the flash mixing.

**Key words.** stars: evolution – subdwarfs – binaries(including multiple): close

## 1. Introduction

In the Hertzsprung-Russell diagram (HRD), subdwarf B (sdB) stars are located between the upper main sequence (MS) and the white dwarf (WD) cooling sequence at the blueward extension of the horizontal branch. They are also known as extreme horizontal-branch (EHB) stars in globular clusters (GCs). SdB stars are important in several aspects. The study of their origin significantly improved our knowledge of stellar and binary evolution theory (Geier 2015). Short-period sdB binary systems are candidates of type Ia supernova progenitors (Maxted et al. 2000a, Wang et al. 2009). Many sdB stars show multiperiodic pulsations and those are important objects of asteroseismology study (Charpinet et al. 2010). SdB stars have been used as distance indicators and as a probe to study the Galactic structure and evolution (see the review of Heber 2009, 2016 and Altmann et al. 2004). They are also considered to be crucial sources of far-

ultraviolet radiation in early-type galaxies (Ferguson et al. 1991; Brown et al. 2000; Han et al. 2007) since they are hot (with effective temperature  $T_{\text{eff}}$  between 20000-40000 K) and have relatively long lifetimes ( $\sim 10^8$  yr).

SdB stars are generally believed to be helium-core-burning stars with extremely thin hydrogen envelopes ( $< 0.02 M_{\odot}$ ). More than half of them are found in binaries (Maxted et al. 2001; Napiwotzki et al. 2004; Copperwheat et al. 2004). Han et al. (2002, 2003) developed a detailed binary model for the formation of sdBs, which successfully explains field sdBs and possibly EHB stars in GCs (Han 2008). In the binary scenario, there are three formation channels for sdBs, i.e. stable Roche lobe overflow (RLOF) for those with long orbital periods, common envelope (CE) ejection for those with short orbital periods, and the merger of helium white dwarf (WD) for single sdBs.

The key point of the three channels above is the He ignition in the core. In most instances, the He core is degenerate and the

He ignition is explosive, i.e. there are several He flashes before the stable He core burning is established. Due to numerical difficulties in dealing with flashes in most of stellar evolution codes, almost all the sdB models are artificially constructed from relatively massive stars with non-degenerate cores (e.g. Brown et al. 2001; Han et al. 2002). The constructed sdB stars generally have the same core mass as that in the progenitors at the He ignition, but the composition in the envelope may be different based on different assumptions. The He flashes may alter envelope mass and element abundances (Brown et al. 2001, Sweigart et al. 2004). A detailed study on the He flash process before the stable He-core burning is necessary and important for our understanding of the characteristics of sdB stars and for the study of asteroseismology. The newly developed stellar evolution code MESA (Modules for Experiments in Stellar Astrophysics, Paxton et al. 2011, 2013, 2015) can resolve dramatic changes such as flashes in stellar evolution, then provide a good opportunity for studying the characteristics of sdBs in details.

Schindler et al. (2015) constructed a series of sdB models using MESA. These models reproduced the general properties of the zero-age EHB and the interior structures of sdB stars from the asteroseismology. The origin of sdB stars is ignored in their study, which may play a crucial role in the structure of sdB stars, especially for the mass and composition in the envelope. For example, sdB stars from stable RLOF are considered to have larger envelope mass than those from the CE ejection channel (Han et al. 2002). This envelope mass may further affect the He flash process and the final envelope mass and composition of sdB stars. Much evidence shows that most of sdBs are in short orbit-period binaries (Saffer et al. 1998, Jeffery et al. 1998, Koen et al. 1998, Orosz et al. 1999, Moran et al. 1999, Maxted et al. 2000a, 2000b, 2001, Barlow et al. 2013; Kupfer et al. 2015). This means that the CE ejection channel is a major mechanism for producing sdBs.

In this paper, we will employ MESA to systematically study the characteristics of sdBs from the CE ejection channel. In section 2, we simply introduce the basic inputs in the code and the method of simulating the CE process. The results are presented in section 3, where we will see that the sdB stars produced from the CE ejection channel show two distinct groups on the effective temperature-gravity diagram. In section 4, we discuss the influence on the results from the treatment of the CE ejection, mass loss during He flashes and metallicity, and some observationally related objects. A conclusion is given in section 5.

## 2. Stellar Evolution Calculations

We used version 7184 of MESA and adopted the physics options similar to that in the standard model of Schindler et al. (2015), i.e. the element abundances are chosen for population I stars, saying,  $Z = 0.02$  and  $X = 0.70$  for the metallicity and hydrogen mass fraction, respectively, and the nuclear network is `pp_cno_extras_o18_ne22.net`, in which all reactions for H and He burning are included. The mixing length parameter,  $\alpha_{MLT}$ , is set to 2 and the opacity table is OPAL type II, which allows the abundances of C and O varying with time. For simplicity, no stellar wind or other mass loss is included in our calculations except for the CE ejection.

In the CE ejection channel, the progenitor of an sdB is a giant and fills its Roche lobe near the tip of red giant branch (RGB). The following mass transfer is dynamically unstable and a common envelope forms. The donor's core and the companion spiral in the CE. Due to the friction between the inner binary and the CE, the orbit decays and the orbital energy is released and deposited in the envelope. The envelope may be ejected eventually

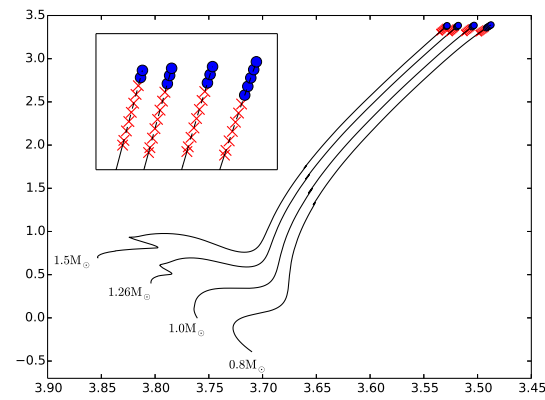


**Fig. 1.** Evolutionary tracks on the Hertzsprung-Russell diagram for the four stars studied in the paper. Symbols of ‘ $\times$ ’ and ‘ $\bullet$ ’ mark the positions where the star fills its Roche lobe and enters into the CE evolution. The symbol ‘ $\times$ ’ are for those having a strong H flash after the main He flash and ‘ $\bullet$ ’ for those without such a strong H flash (see text for the details).

when the released orbital energy is larger than the binding energy of the envelope (Han et al. 2002). The whole process is dynamical (with a timescale of  $\sim 10^3$  yrs, see Ivanova et al. (2013) and references therein), and cannot be simulated by MESA yet. So, we model this process in a way similar to that of Han et al. (2002). We firstly evolve a single star to the position where the CE begins (near the tip of RGB), then artificially remove the envelope with a high mass-loss rate ( $10^{-3} M_{\odot} \text{yr}^{-1}$ ). In general, the giant expands dramatically due to mass loss and contracts suddenly after almost all of the envelope has lost. We stop the mass loss when the star starts to collapse, i.e. the radius of the star,  $R$ , is equal to the initial radius at the beginning of mass loss,  $R_0$ . The evolution of the remnant is followed till the surface temperature is less than 5000 K, that is, the star is evolving to a cool He WD or a carbon-oxygen WD (after a sdB phase).

We adopt four initial stellar masses (the mass donor) for our study, i.e.  $M_i = 0.8M_{\odot}$ ,  $1.0M_{\odot}$ ,  $1.26M_{\odot}$  and  $1.5M_{\odot}$ , respectively. For each mass, we systematically investigate a series of positions where the CE begins on the RGB, i.e. the core mass increases from the minimum mass allowed for He ignition<sup>1</sup> to the tip of RGB, by step of  $0.002M_{\odot}$ . Fig. 1 shows the positions to be studied on the evolutionary tracks. The initial mass and core mass for each point are listed in Table 1.

## 3. Characteristics of sdB Stars from Our Models

### 3.1. Location on the $T_{\text{eff}} - \log g$ diagram

We totally calculated 44 models and all the produced sdBs are presented on the temperature-gravity ( $T_{\text{eff}} - \log g$ ) diagram (Fig. 2), where we see that, for each donor, the produced sdB stars obviously show two groups. One group almost has no H-rich envelope and is crowded at the hottest temperature end of the EHB, very close to zero-age helium main sequence (ZAHeMS, the dot-dashed lines). The other group has significant H-rich envelope and spreads over the whole canonical EHB region. There is a discontinuous increase in the effective temperature at the transition between the two groups, leaving a gap on  $T_{\text{eff}} - \log g$  dia-

<sup>1</sup> If the core mass at the onset of the CE is less than the minimum mass, helium cannot be ignited and the remnant will evolve to a He WD directly (see Han et al. 2002).

**Table 1.** Properties of sdB stars produced from the CE ejection channel in our study. The first three columns show the initial mass of the donors  $M_i$ , the core mass at the onset of the CE process  $M_c$ , and the remnant mass after the CE process  $M_{\text{sdB}}$ , respectively. The 4-6th columns are the total hydrogen mass  $M_H$ , surface He abundance ( $Y$ ) and surface C abundance ( $X_C$ ), respectively, as He burns stably in the core. The masses are in units of solar mass.

$M_i$	$M_c$	$M_{\text{sdB}}$	$M_H$	$Y$	$X_C$
0.8	0.443	0.453	1.068d-4	0.947	0.020
	0.444	0.454	1.593d-4	0.943	0.021
	0.446	0.456	0.973d-4	0.948	0.023
	0.448	0.458	1.714d-4	0.941	0.025
	0.45	0.461	3.724d-4	0.925	0.027
	0.452	0.463	1.100d-4	0.945	0.029
	0.454	0.465	0.991d-4	0.943	0.034
	0.456	0.467	0.733d-3	0.298	0.003
	0.458	0.470	2.589d-3	0.298	0.003
	0.46	0.472	4.054d-3	0.298	0.003
1.0	0.462	0.473	5.129d-3	0.298	0.003
	0.464	0.476	6.855d-3	0.298	0.003
	0.443	0.450	1.359d-4	0.944	0.019
	0.444	0.451	2.994d-4	0.931	0.021
	0.446	0.453	1.113d-4	0.942	0.022
	0.448	0.455	1.383d-4	0.939	0.023
	0.45	0.457	0.984d-4	0.943	0.026
	0.452	0.459	2.387d-6	0.943	0.028
	0.454	0.462	1.316d-4	0.942	0.031
	0.456	0.463	3.110d-4	0.759	0.018
1.26	0.458	0.466	1.099d-3	0.301	0.003
	0.46	0.468	2.061d-3	0.301	0.003
	0.462	0.470	2.849d-3	0.301	0.003
	0.443	0.449	1.992d-4	0.938	0.019
	0.444	0.450	1.663d-4	0.942	0.020
	0.446	0.452	2.021d-4	0.938	0.023
	0.448	0.454	1.982d-4	0.941	0.024
	0.45	0.456	3.228d-4	0.928	0.025
	0.452	0.458	1.782d-4	0.940	0.027
	0.454	0.459	1.539d-4	0.941	0.029
1.5	0.456	0.461	1.752d-4	0.938	0.033
	0.458	0.463	0.732d-3	0.299	0.003
	0.46	0.465	1.981d-3	0.299	0.003
	0.462	0.467	3.192d-3	0.299	0.003
	0.445	0.449	1.406d-4	0.943	0.021
	0.446	0.450	1.918d-4	0.939	0.022
	0.448	0.452	3.265d-4	0.928	0.023
	0.45	0.454	1.877d-4	0.940	0.024
	0.452	0.456	1.949d-4	0.939	0.026
	0.454	0.458	1.527d-4	0.941	0.028

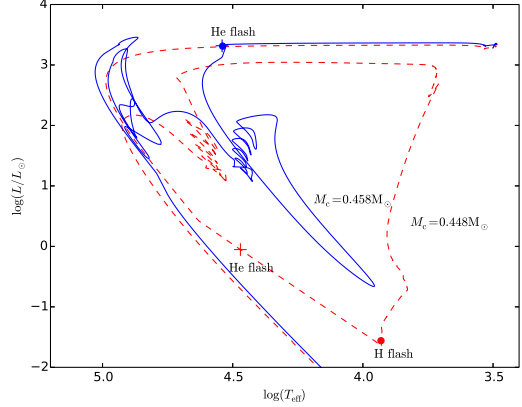


**Fig. 3.** Typical evolutionary tracks (starting from the end of the CE ejection) for the two groups of sdBs produced from the CE ejection channel. The two models have the same initial masses ( $M_i = 0.8M_\odot$ ), but different core masses at the onset of the CE ejection, that is,  $M_c = 0.448M_\odot$  for that of the flash-mixing sdB (the dashed line) and  $0.458M_\odot$  for that of the canonical sdB (the solid line), respectively. Symbols ‘+’ and ‘•’ show the positions where the first He and H flash occur, respectively.

the sdB properties. For convenience, we refer the first class as the flash-mixing sdBs and the second as the canonical sdBs.

The observed sdB binaries with short-orbital periods (Maxted et al. 2001; Kupfer et al. 2015) are presented in Fig. 2 for comparison. We see that most sdBs can be reproduced by the canonical sdBs, but several sdBs are located in the blue extending of the canonical sdBs i.e. some are in the gap between the two groups and some are on the flash-mixing sdB tracks, but the number density is obviously lower than that in the canonical sdB region. We will give some discussions on this in section 4.1.

### 3.2. Origin of the Dichotomy of sdB Properties

For each group of sdBs, we choose one typical model to see the details during He flashes. The model for the flash-mixing sdBs has an initial mass of  $0.8M_\odot$  and a core mass of  $0.448M_\odot$  at the onset of the CE ejection. The model for the canonical sdBs has the same initial mass but a core mass of  $0.458M_\odot$  at the onset of CE ejection. Fig. 3 shows their evolutionary tracks after the CE ejection on the HRD and the positions where the first He and H flashes occur.

The flash-mixing model is shown as the red dashed line in Fig. 3. We see that, for this model, the first He flash occurs when the star is descending along the WD cooling sequence and is followed by a very strong H flash. The He- and H-burning luminosity during the flashes are presented in Fig. 4, where the structure of convection near the surface is also presented to understand the surface composition of the products, then their positions on HRD. From Fig. 4 we see that, the convection has developed during the He flash and penetrates into the H-rich envelope (the H-rich boundary is defined as that with H abundance  $X = 0.1$ ). Most of the H-rich matter has been involved into the hot helium-burning interior and is ignited. So we see an extra strong H flash following the He flash. The maximum luminosity of the H flash is  $L_H \sim 10^{10}L_\odot$ , even larger than that of the He flash. As a result, the H-rich material is nearly exhausted and the remnant is almost a naked He core. All the flash-mixing sdBs have similar processes during the first He flash and crowd at the hottest temperature end of the EHB, very close to ZAHeMS.

gram. Only two products are found to be located in the gap from our models. The products in the first group have higher He and C abundances in the envelope than those in the second group (Table 1). In the following, we will see that it is the convection developed during the first He flash that causes the dichotomy of

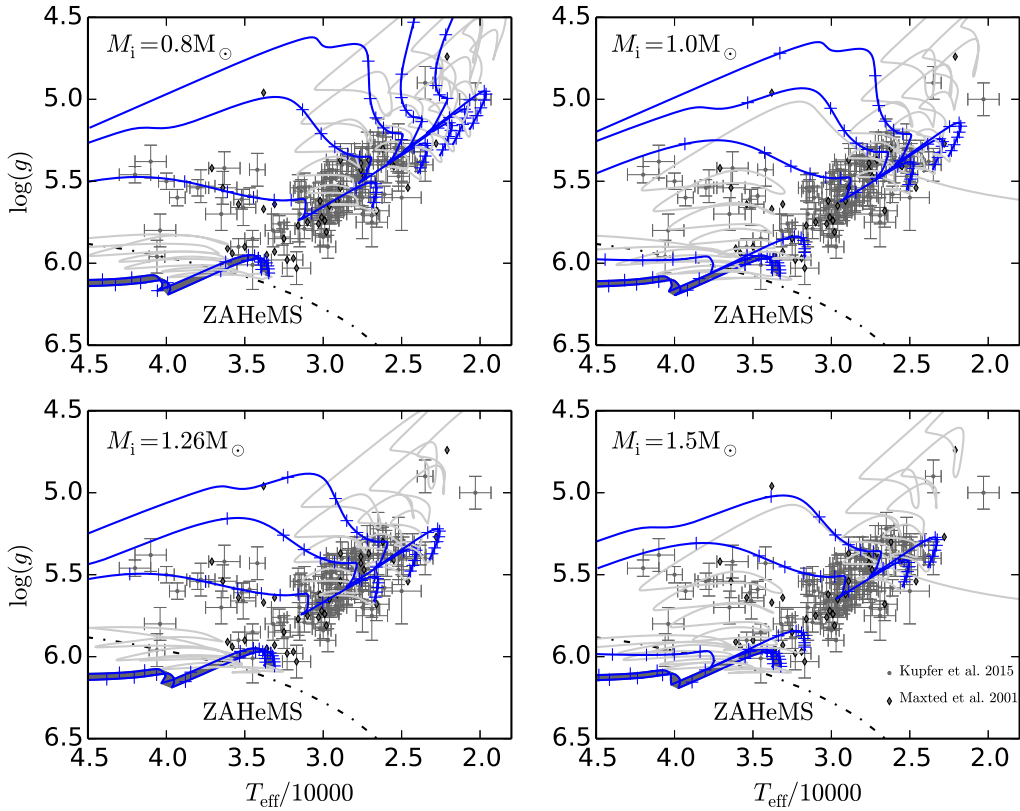


**Fig. 2.** Evolutionary tracks of the produced sdB stars on the effective temperature-gravity ( $T_{\text{eff}}$  –  $\log(g)$ ) diagram. Initial stellar mass,  $M_i$ , and the position of zero-age helium main sequence (ZAHeMS, the dot-dashed line) are indicated in the figure. The shaded area between the lowest two lines in each panel shows the region of the evolutionary tracks of the flash-mixing models occupied (see the text for details) for clarity. The age difference between adjacent crosses is  $10^7$  yr. The dots and diamonds are short orbital-period sdBs from Maxted et al (2001) and Kupfer et al. (2015), respectively. The grayish lines are the tracks during helium flashes before stable He-core burning.

For the canonical model (the blue solid line in Fig. 3), however, the first He flash occurs much earlier, i.e. when the star is approaching to the maximum temperature after the CE ejection, and the convection region developed in the flash never penetrates into the H-rich envelope (see Fig. 5). So, the H-rich matter has not involved in the hot helium burning region and the strong H flash appeared in the flash-mixing model never occurs in this model. The H-burning is moderate in the envelope and significant H-rich material has been left when the stable He-core burning is established. The sdBs produced in this way spread over the whole sdB region and the exact location on the  $T_{\text{eff}}$  –  $\log(g)$  diagram is related to the H-rich envelope mass left, as studied in previous (Heber 2016).

Whether the temporary convection induced by the first He flash penetrates into the H-rich envelope or not depends on the position at which the first He flash occurs, as discussed by Brown et al. (2001). If the first He flash occurs just after the end of mass loss (due to a strong wind, the CE ejection or Roche lobe overflow), i.e. when the star is approaching to the maximum temperature or near the top of the WD cooling sequence, a high entropy barrier at the bottom of the H-rich envelope prevents the convection penetrating into the envelope. With the star descending on the WD cooling curve, however, the entropy barrier becomes lower and lower and the convection can penetrate into the envelope easily (see also Iben 1984, Castellani & Castellani 1993, D'Cruz et al. 1996, Lanz et al. 2004). This leads to the

dichotomy of sdB properties and a discontinuous increase in  $T_{\text{eff}}$  between the two classes, leaving a gap on the  $T_{\text{eff}}$  –  $\log(g)$  diagram, as presented in Fig. 2.

The mixing between the core and the H-rich envelope may be complete or incomplete. This further divides the flash mixing into two subtypes, i. e. deep mixing and shallow mixing, as shown by Sweigart et al. (2004), where the products with deep mixing are similar to that of the flash-mixing sdBs in our study and those with shallow mixing are located in the gap between the flash-mixing sdBs and the canonical sdBs. Two models in our calculation, i.e.  $M_i = 1.0 M_{\odot}$ ,  $M_c = 0.456 M_{\odot}$  and  $M_i = 1.5 M_{\odot}$ ,  $M_c = 0.458 M_{\odot}$ , are located in the gap (see Fig. 2). Their behaviors on the HRD are similar to that of the canonical sdBs in Fig. 3 except that the first He flash occurs when the stars have entered into the WD cooling sequence but still hot enough. The temporal evolution of the H- and He-burning luminosity and convection region during the He flashes for the model of  $M_i = 1.0 M_{\odot}$ ,  $M_c = 0.456 M_{\odot}$  are presented in Fig. 6. We see that the convection induced by the first He flash penetrates into the H-rich envelope but much later than that in Fig. 4, i.e. the penetrating occurs when the first He flash is extinct. In this case, the H-rich material has in fact not been involved into a high-temperature region to be consumed. In the following series of He flashes, the convection region never penetrates the H-rich envelope again. The products with shallow mixing then have surface H abundance

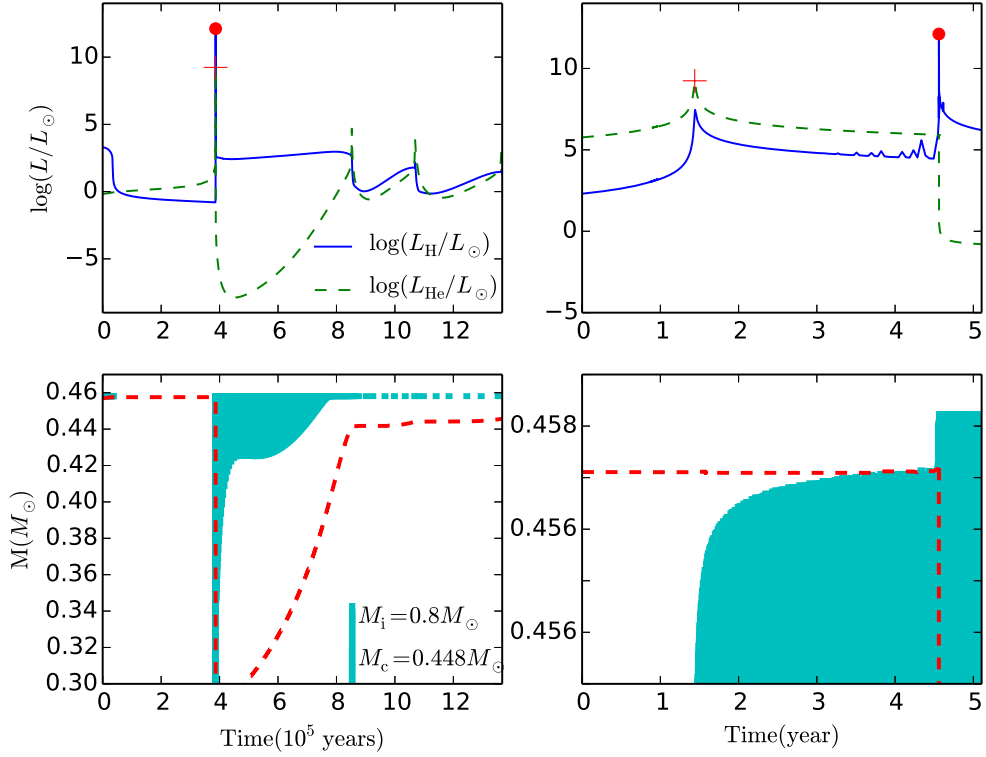


**Fig. 4.** Temporal evolution of the H- and He-burning luminosity (the upper panels) and the structure of convection region (the shaped region) near the surface (the bottom panels) during the flashes. The model has  $M_i = 0.8M_\odot$  and  $M_c = 0.448M_\odot$  at the onset of the CE ejection. Symbols '+' and '•' show the positions where the first He and H flash occur, respectively (see Fig. 3). The dashed line in the bottom panels is the boundary of the H-rich envelope, that is, the H mass abundance of  $X_H = 0.1$ . We see that the convection developed during the first He flash penetrates into the H-rich envelope, resulting in an extra very strong H flash. The right two panels zoom in the first He and H flashes.

between that of deep mixing and that of the canonical sdBs, and stay in the gap between the two classes.

## 4. Discussions

### 4.1. The Modelling of the CE Ejection Process

In our study, we mimic the CE ejection process using a very high mass-loss rate ( $10^{-3}M_\odot\text{yr}^{-1}$ ) and stop the ejection process when the star begins to collapse, i.e. the radius of the star,  $R$ , is equal to the initial radius at the beginning of mass loss,  $R_0$ . Though this modelling is physically reasonable, there is still a large uncertainty due to the lack of detailed dynamical simulations. The mass of the envelope, which is determined by the endpoint of the ejection process, is a key factor that can alter the properties of the produced sdBs, since it is related to the development of convection region during the He flashes. So, when the CE ejection process terminates becomes very important here. In this subsection, we will do some examinations on this by artificially fixing the remnant mass after the CE ejection process, i.e. the ejection process is stopped when the star has a mass equal to a specified value. The examined star has an initial mass of  $M_i = 1.0M_\odot$  and a core mass of  $M_c = 0.446M_\odot$  at the onset of the CE ejection. The produced sdB is a flash-mixing sdB with a mass of  $0.453M_\odot$  from our study in Section 3 (the standard model hereinafter). Various stellar masses after the CE ejection process are adopted, i.e.  $M_{\text{sdb}} = 0.452 - 0.472M_\odot$  by step of  $0.002M_\odot$ . The results are shown in Fig. 7, where the products crowd at the hottest end

of EHB when  $M_{\text{sdb}} = 0.452 - 0.466M_\odot$ , and spread over the canonical sdB region when  $M_{\text{sdb}} \geq 0.468M_\odot$ . This means that it is the envelope mass (or the position at which the CE ejection terminates) that determines the place of the produced sdBs on the  $T_{\text{eff}} - \log g$  diagram. Our study shows that, for a given initial stellar mass and a given core mass at the onset of the CE, if the CE ejection stops earlier, the star has an envelope more massive. The product is then a canonical sdB more likely, and vice versa.

The fact that very few short-orbital-period sdB binaries are located on or near the flashing-mixing sdB tracks as mentioned in Section 2 suggests that the envelope mass after the CE ejection is probably more massive than that expected before. In general, we consider that the ejection stops when the donor contracts back into its Roche Lobe,  $R_L$ . The value of  $R_L$  is  $\approx R_0$  at the onset of the CE and decreases with the ejection process. The assumption that the ejection ends as  $R < R_0$  is therefore an upper limit and gives the maximum envelope mass left on the remnant. A falling back process, similar to that happened in nova, probably occur in the CE ejection and provides an appropriate way of increasing the envelope mass. The detailed process is beyond of the scope of this paper.

### 4.2. The Mass Loss during Flashes

In our study, we have not included any mass loss process except for the CE ejection for simplicity. However, the star obviously loses some material when it evolves on the RGB or during strong flashes. The stellar wind on the RGB may change orbit parame-

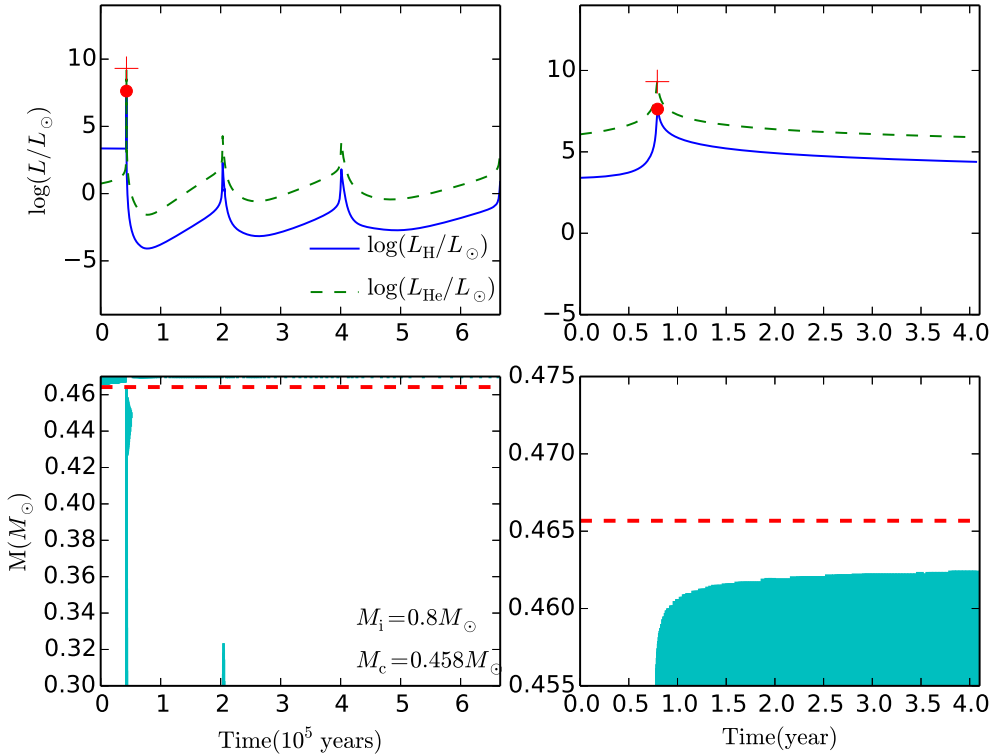


**Fig. 5.** Similar to Fig. 4, but for  $M_i = 0.8M_\odot$ ,  $M_c = 0.458M_\odot$ . The convection developed during the He flashes never penetrates into the H-rich envelope and the strong H flash appeared in Fig. 4 does not appear here.

ters of sdB binaries such as the orbital period, but unlikely affect the properties of the sdB stars, which are determined by the following evolution after the envelope is stripped. The mass loss during the flashes will reduce the envelope's mass of a pre-sdB star, then alters its final position on the  $T_{\text{eff}} - \log(L)$  diagram when stable He-core burning begins. There are two ways of mass loss during the flashes, a strong stellar wind driven by the violent flashes and Roche lobe overflow when the pre-sdB star expands to exceed its Roche lobe radius. The effect of mass loss on the sdB mass is negligible since the mass loss is too small in comparison to  $M_{\text{sdB}}$ , but the effect on the envelope mass may be significant since the envelope mass is itself very small. The mass loss is expected to be larger for the flash-mixing sdBs than that for the canonical sdBs due to the extra strong H flash after the first He flash. For the flash-mixing sdBs, the surface He and C abundance presented in Table 1 may be further enhanced, but their locations on the  $T_{\text{eff}} - \log(L)$  diagram will not change a lot since those objects have had nearly H-exhausted envelope. For the canonical sdBs, the mass loss reduces the envelope mass and the tracks will move towards the lower left on the  $T_{\text{eff}} - \log(L)$  diagram.

#### 4.3. Effect of Metallicity

All the studies above are for Population I stars ( $Z = 0.02$ ). Here we will show some models for  $Z = 0.004$  to see the effect of metallicity on the final results. The star has an initial mass of  $1.0M_\odot$  and various core masses at the onset of the CE process (see Table 3). The results are shown in Fig. 8, which are very similar to that of Pop I stars except for the exact positions on

**Table 2.** Models investigated for a metallicity of  $Z = 0.004$ . The star has an initial mass of  $1.0M_\odot$ . The first two columns show the core mass at the onset of the CE process  $M_c$ , and the remnant mass after the CE process  $M_{\text{sdB}}$ , respectively. The 3-5th columns are the total hydrogen mass  $M_H$ , surface He abundance ( $Y$ ) and surface C abundance ( $X_C$ ), respectively, as He burns stably in the core. The masses are in units of solar mass.

$M_c$	$M_{\text{sdB}}$	$M_H$	$Y$	$X_C$
0.453	0.460	0.820d-4	0.964	0.015
0.454	0.461	0.916d-4	0.956	0.011
0.456	0.463	1.178d-4	0.959	0.015
0.458	0.465	2.200d-4	0.953	0.014
0.46	0.467	1.304d-4	0.956	0.017
0.462	0.469	0.926d-4	0.952	0.020
0.464	0.471	2.329d-4	0.944	0.023
0.466	0.473	5.177d-4	0.269	0.001
0.468	0.475	1.719d-3	0.269	0.001
0.47	0.478	3.395d-3	0.269	0.001
0.472	0.480	4.759d-3	0.269	0.001

the  $T_{\text{eff}} - \log(L)$  diagram, that is, the produced sdBs appear as two groups, one group crowds at the hottest end of EHB (for  $M_c = 0.453 - 0.456M_\odot$ ) and the other one spreads over the canonical sdB region (for  $M_c \geq 0.466M_\odot$ ). The whole tracks of  $Z = 0.004$  moves lower left on the  $T_{\text{eff}} - \log(L)$  diagram. This also indicates that the observed sdBs in the gap between the flash-mixing sdBs and the canonical sdBs can be well understood by adopting various metallicities.

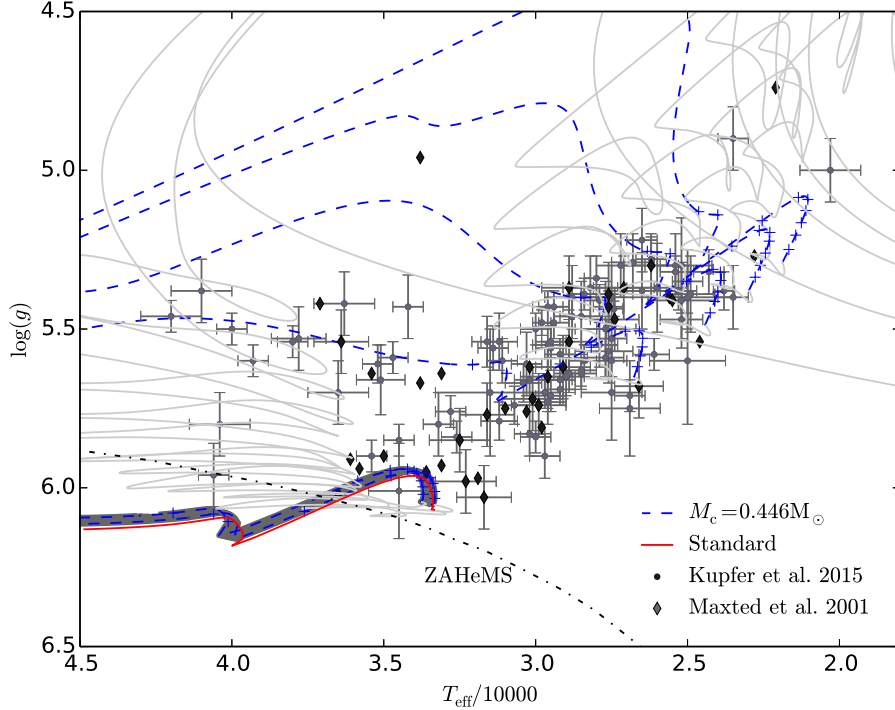


**Fig. 7.** Evolutionary tracks of the produced sdB stars from the star with an initial mass of  $1.0M_{\odot}$  and a core mass of  $0.446M_{\odot}$ . The sdB mass,  $M_{\text{sdB}}$ , is artificially set to be equal to  $0.452, 0.454, \dots, 0.472$  and  $0.474M_{\odot}$  (by step of  $0.002M_{\odot}$ ). The products crowd at the hottest end of EHB for  $M_{\text{sdB}} = 0.452 - 0.466M_{\odot}$  (located in the shaded region between the lowest two dashed lines), and spread over the canonical sdB region when  $M_{\text{sdB}} \geq 0.468M_{\odot}$  (from bottom to up,  $M_{\text{sdB}} = 0.468, 0.470, 0.472$  and  $0.474M_{\odot}$ , respectively). The red solid line is for the standard model ( $M_{\text{sdB}} = 0.453$ ). Short orbital-period sdBs from Maxted et al (2001) and Kupfer et al. (2015) are presented in the figure for comparison. The grayish lines are the tracks during helium flashes before stable He-core burning.

#### 4.4. Related to He-rich sdB Stars

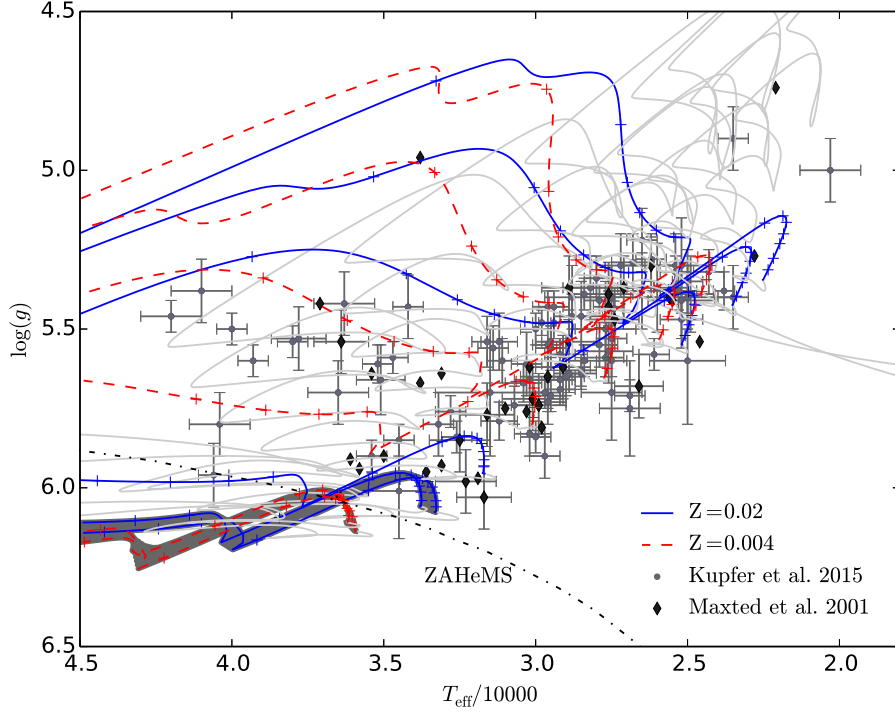
Since He and C have been enhanced in the envelope during the flash mixing (see Table 1), the flash-mixing sdBs may be connected with the He-rich sdB stars. Figs. 9 and 10 show the comparisons of our models with the observations in the  $T_{\text{eff}} - [\text{He}/\text{H}]$  diagram and in the  $T_{\text{eff}} - [\text{C}/\text{H}]$  diagram, respectively. The observed atmospheric parameters of sdBs are from Péter et al. (2012), who divides the sample into three types according to the ratio of He to H abundance,  $\log(n_{\text{He}}/n_{\text{H}})$ , i.e. H-rich if  $\log(n_{\text{He}}/n_{\text{H}}) < -0.349$ , intermediate He-rich if  $-0.349 \leq \log(n_{\text{He}}/n_{\text{H}}) \leq 0.6$  and He-rich if  $\log(n_{\text{He}}/n_{\text{H}}) > 0.6$ . From Fig. 9, we see that the flash-mixing sdBs (the diamonds) have similar surface abundances to that of intermediate He-rich and He-rich sdB stars while the canonical sdBs (the stars) are located near the boundary separating the H-rich and intermediate He-rich sdBs. Note that, with the sdBs evolving, the effective temperature increases and the surface He abundance probably reduces if the gravity setting is considered. The theoretical models then move left downwards, that is, the flash-mixing models may go across the intermediate He-rich and He-rich samples and the canonical models will go across the H-rich samples.

Figure. 11 presents the sdB samples on the  $T_{\text{eff}} - \log(g)$  diagram, comparing with the theoretical evolutionary tracks. The figure shows that the intermediate He-rich and He-rich sdBs are indeed spreading around the evolutionary tracks of flash-mixing models, further indicating that most of the (intermediate) He-rich stars can be well understood by the flash mixing (see also Miller et al. 2008). In particular, the flash-mixing sdBs originated from

the CE ejection channel are in short-orbital periods and should be responsible for (intermediate) He-rich sdBs with short orbital periods. However, only one intermediate He-rich sdB, CPD-20°1123, has been found in short orbital period (Naslim et al. 2012), and its location on the  $T_{\text{eff}} - \log(g)$  diagram seems not relevant to the flash-mixing model. The lack of He-rich sdBs in short-orbital periods further indicates that the flash mixing unlikely happens in the products of the CE ejection, probably due to relatively massive envelope mass resulted from a falling back process after the CE ejection, as discussed in section 4.1.

#### 4.5. Related to Blue Hook Stars in GCs

Blue hook stars occupy a very blue position on the HB but with fainter luminosity than normal EHB stars. Their formation mechanism is not very clear. Brown et al. (2001) suggested that the late hot He flash happened as the star is descending the WD cooling curve can reproduce such objects. In their study, the progenitors undergo unusually huge mass loss on the RGB and the products are constructed based on some assumptions due to the numerical difficulties in dealing with the He flashes. Employed tidally enhanced stellar wind in binaries, Lei et al. (2015) reproduced the blue hook stars in NGC 2808. The evolutions after the mass loss are very similar to that shown in this paper since the remnants have very similar structures regardless of the mass stripping way (e.g the CE ejection or strong stellar wind). Our study then provides a new way to forming the blue hook stars in GCs. Furthermore, sdB stars from stable mass transfer may also have similar processes if the envelope mass is small enough. The



**Fig. 8.** Evolutionary tracks of the produced sdB stars on the  $T_{\text{eff}} - \log g$  diagram. The star has an initial mass of  $1M_{\odot}$  with a metallicity of  $Z = 0.004$  (the dashed lines). The products crowd at the hottest end of EHB for the core mass  $M_c = 0.453 - 0.456M_{\odot}$  (located in the shaded narrow region of the lowest two lines), and spread over the canonical sdB region when  $M_c \geq 0.466M_{\odot}$  (from bottom to up,  $M_c = 0.466, 0.468, 0.470$  and  $0.472M_{\odot}$ , respectively). The solid lines are for the results of  $Z = 0.02$  for the star with the same initial mass. The age difference between adjacent crosses is  $10^7$  yr. Short orbital-period sdBs from Maxted et al. (2001) and Kupfer et al. (2015) are presented in the figure for comparison. The grayish lines are the tracks during helium flashes before stable He-core burning.

flash mixing is crucial in all of the suggested formation channels and leads to similar observational properties for the blue hook stars themselves. The hints of their origins probably exist in the orbital parameters such as orbital period if they were in binaries.

## 5. Conclusions

Employing the MESA, we studied the properties of sdBs produced from the CE channel. The stars appear as two distinct groups on the  $T_{\text{eff}} - \log g$  diagram, i.e. the flash-mixing sdBs and the canonical sdBs, as defined in this paper. The flash-mixing sdBs almost have no H-rich envelope and are crowded at the hottest temperature end of EHB, while the canonical sdBs have significant H-rich envelope and spreads over the whole canonical EHB region.

The key factor for the dichotomy of the sdB properties is the development of convection during the first helium flash. For the flash-mixing sdBs, the star enters into the CE process earlier and has a lower He core mass. The first helium flash occurs when the star is descending the WD cooling curve and is followed by a violent hydrogen flash, which is triggered by convective element mixing between H-rich envelope and He-burning region. Hydrogen in the envelope is then almost exhausted and the products are almost naked He cores. For the canonical sdBs, the star enters into the CE process later and has a more massive He core. The first helium flash happens much earlier, and the convection induced by the helium flash never penetrates into the H-rich envelope due to the high entropy barrier of H-rich envelope. The products then remain significant H-rich envelope and spread over

the whole canonical EHB region. Their positions are determined by the H-rich envelope mass as studied in many previous work. Therefore, the dichotomy of the sdB properties from the CE ejection channel is intrinsic and caused by the interior structure of the star after the CE ejection.

The treatment of convection and the modelling of the CE ejection process will change the parameter spaces much for the two typical groups of sdB stars. For a given initial stellar mass and a given core mass at the onset of the CE, if the CE ejection stops earlier, the star will be more massive and have a more-massive envelope. The produced sdB is a canonical sdBs more likely, and vice versa. The fact that very few short-orbital period sdB binaries are located in the flash-mixing sdB region means that the sdBs produced from the CE ejection have more massive envelope mass than expected. The lack of short-orbital-period He-rich sdBs also indicates that the flash mixing is rare in the products of the CE ejection. A falling back process after the CE ejection, similar to that happened in nova, is an appropriate way of increasing the envelope mass, then prevents the flash mixing.

There is a discontinuous increase in the effective temperature at the transition between the two groups, leaving a gap on the  $T_{\text{eff}} - \log g$  diagram. Only two products are found to be in the gap from our model grid. The properties of the two models are consistent with that of shallow mixing (mixing is incomplete) and can well explain the blue hook stars in NGC 2808. Various formation scenarios for blue hook stars give similar characteristics of such objects, and the hints of their origins probably exist in the orbital parameters if they were in binaries.

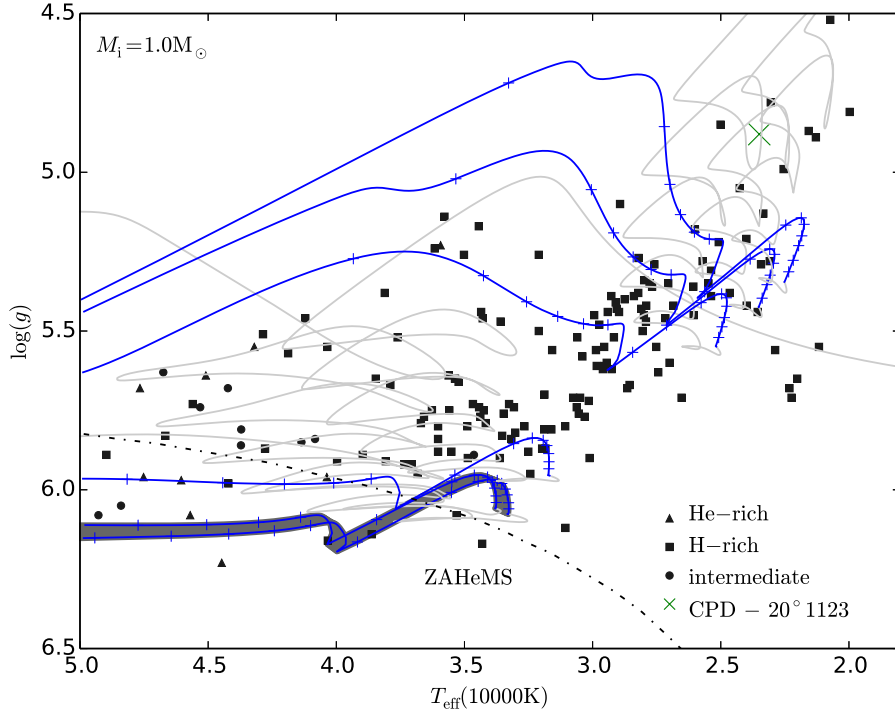


**Fig. 11.** Evolutionary tracks of the produced sdBs and the sdB samples with atmospheric He abundance (Péter et al. 2012) on the effective temperature-gravity diagram. The shaded area between the lowest two lines is the region of the evolutionary tracks of the flash-mixing models occupied. The age difference between adjacent crosses on the evolutionary tracks is  $10^7$  yr. The symbol 'x' is for CPD-20°1123, an intermediate He-rich sdB with an orbital period of 2.3698 d (Naslim et al. 2012). The grayish lines are the tracks during helium flashes before stable He-core burning.

**Acknowledgements.** This work is supported by the Natural Science Foundation of China (Nos. 11173055, 11422324, 11521303, 11390374), by Yunnan province (Nos. 2012HB037, 2013HA005) and by the Chinese Academy of Sciences (No. KJZD-EW-M06-01).

## References

Altmann, M., Edelmann, H., & de Boer, K. S. 2004, A&A, 414, 181  
Barlow, B., Wade, R. A., & Liss, S. 2013, American Astronomical Society Meeting Abstracts #221, 221, 142.17  
Brown, T. M., Bowers, C. W., Kimble, R. A., Sweigart, A. V., & Ferguson, H. C. 2000, ApJ, 532, 308  
Brown, T. M., Sweigart, A. V., Lanz, T., Landsman, W. B., & Hubeny, I. 2001, ApJ, 562, 368  
Brown, T. M., Sweigart, A. V., Lanz, T., Landsman, W. B., & Hubeny, I. 2001, ApJ, 562, 368  
Castellani, M., & Castellani, V. 1993, ApJ, 407, 649  
Charpinet, S., Green, E. M., Baglin, A., et al. 2010, A&A, 516, L6  
Copperwheat, C. M., Morales-Rueda, L., Marsh, T. R., Maxted, P. F. L., & Heber, U. 2011, MNRAS, 415, 1381  
D'Cruz, N. L., Dorman, B., Rood, R. T., & O'Connell, R. W. 1996, ApJ, 466, 359  
Ferguson, H. C., Davidsen, A. F., Kriss, G. A., et al. 1991, ApJ, 382, L69  
Geier, S. 2015, Astronomische Nachrichten, 336, 437  
Han, Z., Podsiadlowski, P., Maxted, P. F. L., Marsh, T. R., & Ivanova, N. 2002, MNRAS, 336, 449  
Han, Z., Podsiadlowski, P., Maxted, P. F. L., & Marsh, T. R. 2003, MNRAS, 341, 669  
Han, Z., Podsiadlowski, P., & Lynas-Gray, A. E. 2007, MNRAS, 380, 1098  
Han, Z. 2008, A&A, 484, L31  
Heber, U. 2009, ARA&A, 47, 211  
Heber, U. 2016, PASP, 128, 082001  
Iben, I., Jr. 1984, ApJ, 277, 333  
Ivanova, N., Justham, S., Chen, X., et al. 2013, A&A Rev., 21, 59  
Jeffery, C. S., & Pollacco, D. L. 1998, MNRAS, 298, 179  
Koen, C., Orosz, J. A., & Wade, R. A. 1998, MNRAS, 300, 695  
Kupfer, T., Geier, S., Heber, U., et al. 2015, VizieR Online Data Catalog, 357, 669  
Lanz, T., Brown, T. M., Sweigart, A. V., Hubeny, I., & Landsman, W. B. 2004, ApJ, 602, 342  
Lei, Z., Chen, X., Zhang, F., & Han, Z. 2015, MNRAS, 449, 2741  
Maxted, P. F. L., Marsh, T. R., & North, R. C. 2000, MNRAS, 317, L41  
Maxted, P. F. L., Moran, C. K. J., Marsh, T. R., & Gatti, A. A. 2000, MNRAS, 311, 877  
Maxted, P. F. L., Heber, U., Marsh, T. R., & North, R. C. 2001, MNRAS, 326, 1391  
Miller Bertolami, M. M., Althaus, L. G., Unglaub, K., & Weiss, A. 2008, A&A, 491, 253  
Moran, C., Maxted, P., Marsh, T. R., Saffer, R. A., & Livio, M. 1999, MNRAS, 304, 535  
Napiwotzki, R., Karl, C. A., Lisker, T., et al. 2004, Ap&SS, 291, 321  
Naslim, N., Geier, S., Jeffery, C. S., et al. 2012, MNRAS, 423, 3031  
Orosz, J. A., & Wade, R. A. 1999, MNRAS, 310, 773  
Paxton, B., Bildsten, L., Dotter, A., et al. 2011, ApJS, 192, 3  
Paxton, B., Cantiello, M., Arras, P., et al. 2013, ApJS, 208, 4  
Paxton, B., Marchant, P., Schwab, J., et al. 2015, ApJS, 220, 15  
Németh, P., Kawka, A., & Vennes, S. 2012, MNRAS, 427, 2180  
Saffer, R. A., Livio, M., & Yungelson, L. R. 1998, ApJ, 502, 394  
Schindler, J.-T., Green, E. M., & Arnett, W. D. 2015, ApJ, 806, 178  
Sweigart, A. V., Lanz, T., Brown, T. M., Hubeny, I., & Landsman, W. B. 2004, Ap&SS, 291, 367  
Wang, B., & Han, Z. 2009, A&A, 508, L27

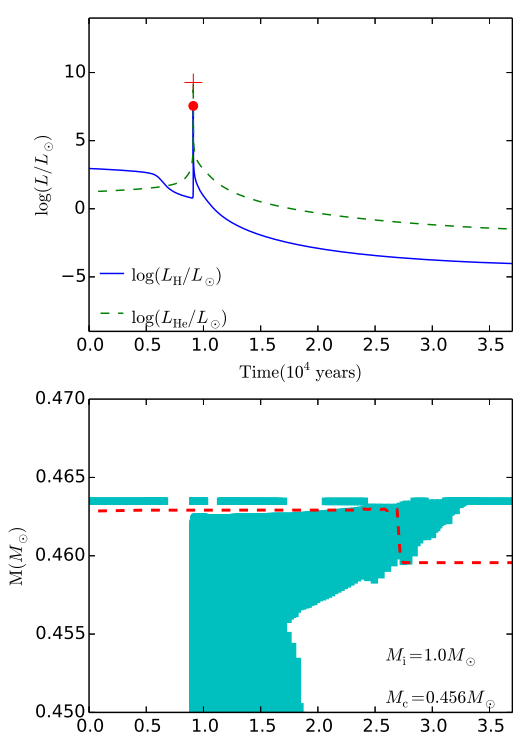


**Fig. 6.** Similar to Fig. 4, but for the first He and H flashes for the model of  $M_i = 1.0 M_\odot$ ,  $M_c = 0.456 M_\odot$ .

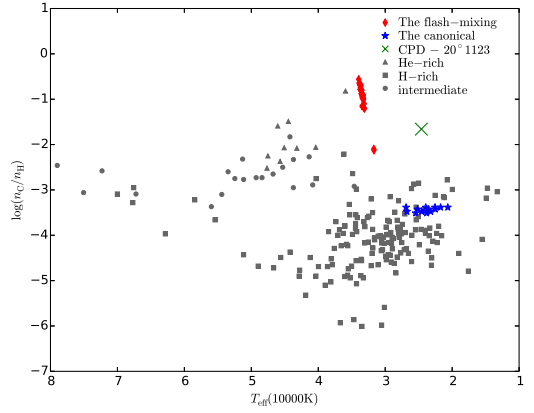


**Fig. 10.** Similar to Fig. 9, but for  $[C/H]$ .

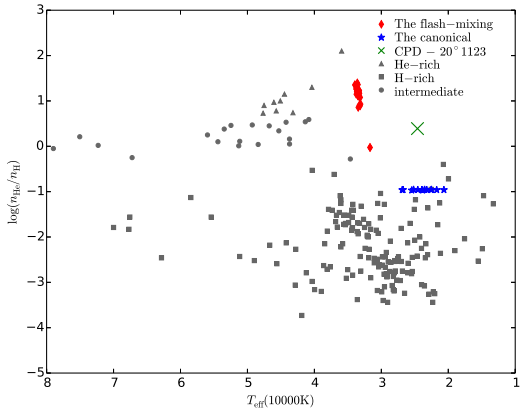


**Fig. 9.** The ratio of He to H abundance at the surface related to the solar value,  $[He/H]$ , versus effective temperature, for our theoretical models and the observations. The sdB samples are from Péter et al.(2012) and have been divided into three types, i.e. H-rich, intermediate He-rich and He-rich, as indicated in the figure. The diamonds are for the flash-mixing sdBs and the stars are for the canonical sdBs, where the He and H abundances are chosen at the onset of stable helium-core burning. The symbol 'x' is for CPD-20°1123, an intermediate He-rich sdB with an orbital period of 2.3698 d (Naslim et al. 2012 ).